Realization of Reliable Solid-State Quantum Memory for Photonic Polarization Qubit

Zong-Quan Zhou, Wei-Bin Lin, Ming Yang, Chuan-Feng Li,* and Guang-Can Guo

Key Laboratory of Quantum Information, University of Science and Technology of China, CAS, Hefei, 230026, China

(Received 17 February 2012; published 10 May 2012)

Faithfully storing an unknown quantum light state is essential to advanced quantum communication and distributed quantum computation applications. The required quantum memory must have high fidelity to improve the performance of a quantum network. Here we report the reversible transfer of photonic polarization states into collective atomic excitation in a compact solid-state device. The quantum memory is based on an atomic frequency comb (AFC) in rare-earth ion-doped crystals. We obtain up to 0.999 process fidelity for the storage and retrieval process of single-photon-level coherent pulse. This reliable quantum memory is a crucial step toward quantum networks based on solid-state devices.

DOI: 10.1103/PhysRevLett.108.190505 PACS numbers: 03.67.Hk, 03.67.Pp, 42.50.Ex, 42.50.Md

Quantum communication channels are naturally carried by photons. To realize a quantum network, we must coherently transfer quantum information between the stationary qubits and the flying photon qubits [1,2]. Despite some remarkable efforts in quantum networks based on cold atoms [3–6], single atom in a cavity [7] Bose-Einstein condensate [8], atomic vapors [9,10] and trapped ions [2,11], there are strong motivations for using more practical systems, e.g., solid-state devices. Rare-earth (RE)-ion-doped solids provide a particular electronic structure that can be seen as a frozen gas of atoms, they have excellent coherence properties for optical and spin transitions. Moreover, they have already shown excellent capability to store light for extended periods [12] with high efficiency [13] and a large bandwidth [14–16]. Recent achievements include the storage of photonic time-bin entanglement generated through spontaneous parametric down conversion (SPDC) [16,17].

Logical qubits with photons can be encoded in several ways, for example, via polarization, time-bin, path, phase or photon-number encodings. The polarization degree of freedom is particularly useful because it allows a single-photon qubit to be transmitted in a single spatial and temporal mode. Polarized photons are more easily transportable qubits and are more robust against decoherence. Note that many quantum light sources generate entangled photons with information encoded in their polarization degree, such as the eight-photon entangled state generated by SPDC [18] and the on-demand entangled photon pairs generated by biexciton decay in quantum dots [19]. Realizing the quantum interface between quantum memory and other quantum light source will also require the capability of the quantum memory to store the polarization information for light. Therefore, the ability to store polarization information with high fidelity is of particular interests. One approach to realizing a polarization-qubit memory is to first transform the polarization encoding into path encoding and then store it into two distant ensembles. This approach has been implemented in both atomic ensembles [3,4,6] and atomic vapors [20]. The above-mentioned realizations suffer from several practical drawbacks due to the extra step of spatially splitting the input state. Phase locking of the two optical paths [6] may be required, and imperfect spatial mode matching may limit the memory fidelity. Another approach is using uniformly absorbed samples for two orthogonal polarizations, which requires no spatially splitting of the input photon. This approach has been implemented with two spatially overlapped atomic ensembles [5], BEC [8] and with a single-atom in a cavity [7]. Up to now, the best fidelity performance achieved with single-photon-level input is 0.95 [8]. All of these experiments are based on the Raman process or electromagnetically induced transparency (EIT). These processes require a strong control or read light pulse during the memory sequence, which introduces unavoidable noise into the retrieval signal.

AFC is an alternative protocol for realizing quantum memory without a strong control light during the memory sequence. AFC quantum memory with RE doped solids has shown an excellent capability to store quantum light [14–17,21–23]. Because of the strongly polarization-dependent absorption of ions in crystal, however, all previous experiments have been conducted with a single predefined polarization. Here, we use an alternative approach to realize AFC quantum memory for polarization-encoded single photons. Two pieces of crystals are used to absorb the orthogonal polarized components that are in the same optical path but at different sites.

The hardware of our quantum memory, which is shown in Fig. 1(a), is composed of two pieces of Nd^{3+}:YVO_4 crystals (doping level 10 ppm) sandwiching a half-wave plate (HWP). The sizes of the two crystals are nearly equal with 1.4 ± 0.01 mm length along the a axis. The $^4I_{9/2} \rightarrow {}^4F_{3/2}$ transition of Nd^{3+} at about 879.705 nm in the Nd^{3+}:YVO_4 crystal shows strong absorption of H polarized photons and little absorption of V polarized photons [24]. Here, H (V) denotes horizontal (vertical), which is defined to be parallel (perpendicular) to the crystal's c axis.

 © 2012 American Physical Society

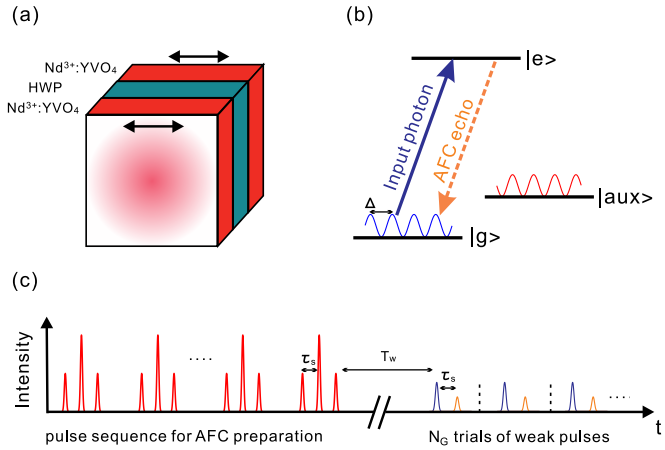

FIG. 1 (color online). (a) Illustration of the sample used as the memory hardware for arbitrary polarizations. The arrows represent the c axis of the crystals. Details about the sample are given in the Supplemental Information [26]. (b) The near 880 nm input photons are absorbed at the ${}^4I_{9/2} \rightarrow {}^4F_{3/2}$ transition of Nd^{3+}. This transition is strongly H polarized. After a programmable time, the photon will be collectively emitted in a desirable spatial mode. (c) The preparation and storage sequence used in the experiment.

This prevents a single piece of Nd^{3+}:YVO_4 crystal from functioning as a polarization-qubit memory because most of the V polarized photons will pass through the crystal without being absorbed. By using a 45° HWP, sandwiched between two parallel Nd^{3+}:YVO_4 crystals, the sample shows nearly equal absorption depth for H, V and arbitrary polarized photons.

The AFC protocol requires a pumping procedure to tailor the absorption profile of an inhomogeneously broadened solid state atomic medium with a series of periodic and narrow absorbing peaks separated by Δ (see Fig. 1). The single input photon is then collectively absorbed by all of the atoms in the comb. The atomic state can be represented by, [25],

$$|1\rangle_A = \sum_j c_j e^{i\delta_j t} e^{ikz_j} |g_1 \ldots e_j \ldots g_N\rangle. \quad (1)$$

Here N is the total number of atoms in the comb; $|g_j\rangle$ and $|e_j\rangle$ represent the ground and excited states, respectively, of atom j; z_j is the position of atom j; k is the wave number of the input field; δ_j is the detuning of the atom frequency and the amplitudes c_j depend on the frequency and on the position of atom j. The atoms at different frequencies will dephase after absorption, but because of the periodic structure of AFC, a rephasing occurs after a time $\tau_s = 2\pi/\Delta$. The photon is reemitted in the forward direction as a result of a collective interference between all of the atoms that are in phase. The collective optical excitation can be transferred into a long-lived ground state to achieve a longer storage time and an on-demand readout [23]. The AFC preparation pulse sequence are shown in Fig. 1(c), in which pulses with temporal width of 40 ns and spacing of τ_s are sent into the sample every 16 μs. In order to obtain the appropriate power spectrum, the central pulse has a field amplitude corresponding to the sum of the amplitudes of the side pulses [14]. The pumping sequences are repeated 300 times to achieve an optimal AFC structure. An experimental AFC structure with a periodicity of 10 MHz is given in the Supplemental Information [26]. The AFC bandwith in our experiment is about 30 MHz which is determined by the temporal width of pump pulses. The AFC bandwidth can be further enlarged with frequency shifted pumping technique [14]. During the storage cycle, N_g trials of single-photon-level coherent pulses are sent into the sample, and the AFC echoes are emitted at a time $2\pi/\Delta$ that is programmed in the pumping procedure. To avoid the fluorescence noise caused by the classical pumping light, the memory cycle begins after waiting for time $T_w = 1.2$ ms after the preparation cycle is completed. The complete pump and probe cycles are repeated at a frequency of 40 Hz.

The experimental setup is shown in Fig. 2. The laser source is a cw Ti:sapphire laser (M Squared, Solstis), and

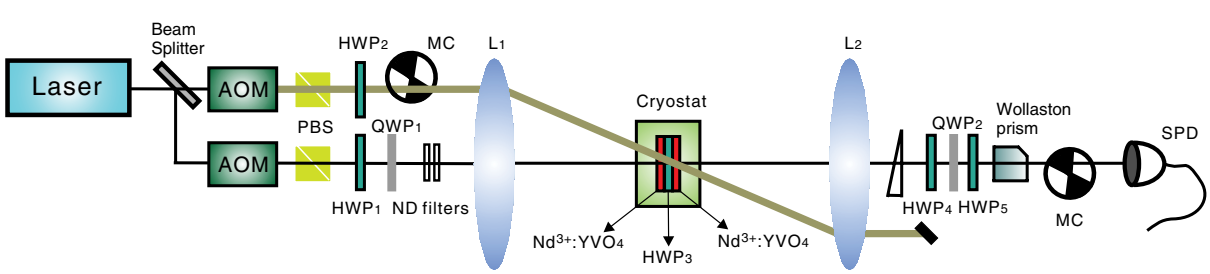

FIG. 2 (color online). The experimental setup for quantum storage of a photonic polarization-qubit in solids. The upper acousto-optic modulators (AOM) produces pump light for the AFC preparation. The lower AOM produces a weak probe light for the storage sequence. The light's polarizations are initialized by the polarization beam splitters (PBS). The probe light's polarizations are controlled by the half-wave plate (HWP_1) and quarter-wave plate (QWP_1). The samples are placed in a cryostat at a temperature of 1.5 K. Beyond the sample, a phase plate (θ) and HWP_4 corrects any polarization rotation caused by the sample. The probe light's polarizations are then analyzed with QWP_2, HWP_5, and a Wollaston prism. The two MCs are used to protect the single-photon detector (SPD) from classical pump pulses.

the laser's wavelength is monitored with a wavelength meter (Bristol 621A). The pump light is generated with a 260 MHz AOM (Brimrose) in a double-pass configuration. To protect the single-photon detectors during the preparation procedure, a mechanical chopper (MC) is placed in the pumping optical path. To achieve a uniform memory efficiency for arbitrary polarized photons, the pumping light should be polarized close to $H + V$. The H polarized light will be mostly absorbed by the first crystal, and the V polarized light will be mostly absorbed by the second crystal, after the polarization rotation by the HWP_3. Carefully adjusting the HWP_2 angle and the pump power can optimize the storage efficiency and balance the efficiency of the H and V components. The photons to be stored are generated by another 260 MHz AOM in double-pass configuration. The AOMs are controlled by an arbitrary function generator (Tektronix, AFG3252). The HWP_1 and QWP_1 prepares input photons with arbitrary polarizations. The input photons are decreased to single-photon level by the neutral density (ND) filters. The storage sequence is repeated 1600 times at a frequency of 1 MHz.

Note that the beam splitters and single mode fiber may degrade the fidelity of the input photons. To achieve a optimum polarization storage performance, we use a setup that differs from those of previous experiments, in which the pump light and probe light have been in counterpropagation or copropagation configurations. The pump light is only overlapped with the probe light at the sample. The pump light and probe light are focused with the same lens L_1 (focal length: 250 mm). This setup achieves a small angle ($\sim$ 15 mrad) between pump and probe lights. The probe light focuses to a diameter of about 100 μm, while the pump light is collimated to produces a much larger diameter on the sample. The sample is placed in a cryostat (Oxford Instruments, SpectromagPT) at a temperature of 1.5 K and with a magnetic field of 0.3 T in the horizontal direction. The applied magnetic field can freeze out magnetic interactions to get a longer coherence time [24]. The two parallel Nd^{3+}:YVO_4 crystals' c-axes are placed in the horizontal direction. The HWP_3 at 45° can exchange H and V polarizations. Because each crystal only strongly absorbs H polarized light, the H polarized input photon is stored in the first crystal, and the V polarized light is stored in the second crystal. Another lens L_2 collects the photons outside of the cryostat. To rotate the polarization back to the input state, another HWP (HWP_4) is placed at 45° outside of the cryostat. Because of the small difference in the lengths of the two crystals, a phase plate is inserted in the optical path to compensate for the small phase shift between H and V polarized photons. The QWP_2, HWP_5 and Wollaston Prism together choose the polarization of the single-photon detections. Another MC is used to protect the single-photon detector (SPD, PerkinElmer, SPCM AQRH-15) from the classical pump light. The signal from the SPD is sent to the time-interval analyzed (TIA) and time-correlated single-photon counting (TCSPC) system (Picoquant, Hydraharp 400).

Figure 3(a) shows an example of weak coherent pulses (the average photon number is 0.8 photons per pulse) with a duration of 60 ns and a polarization of $H + V$ that are collectively mapped onto the sample. A strong echo is emitted after a preprogrammed storage time of 200 ns. The measured storage and retrieval efficiency is about 0.03. The mean input photon number is determined by measuring the detection probability per pulse with the laser 20 GHz off resonance, and take into account the detection efficiency ($\sim$ 0.4) and the transmission from the sample to the detector ($\sim$ 0.6).

To characterize the polarization storage performance of the memory, we perform complete quantum process tomography (QPT) [27,28] on the system (see Supplemental Information [26]). The tomography results of the process matrix χ with a memory time of 200 ns are shown in Fig. 3(b). The results give a process fidelity of 0.999 $\pm$ 0.002 for an average input photon-number of 0.8 photons per pulse. The fidelities of the four input states are 0.995,

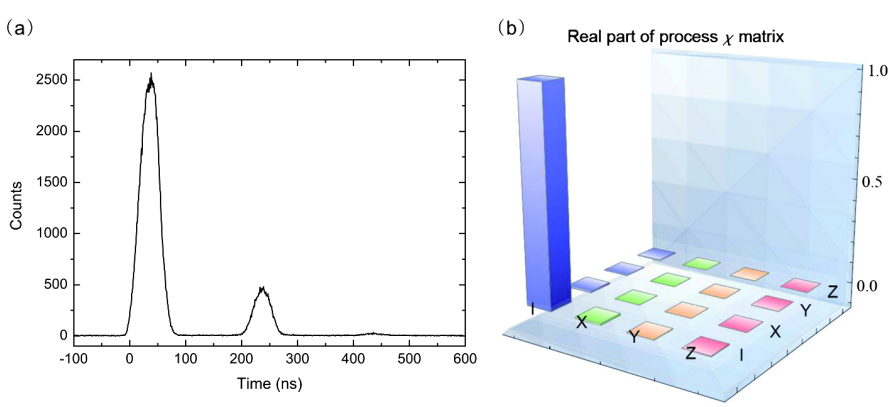

FIG. 3 (color online). (a) With an AFC prepared with a periodicity of 5 MHz, the $H + V$ polarized single-photon pulses are collectively reemitted after a 200 ns storage time in the sample. (b) The real part numbers in the process matrix χ as obtained from a quantum process tomography. All of the imaginary numbers are close to zero, with the largest amplitude being 0.017.

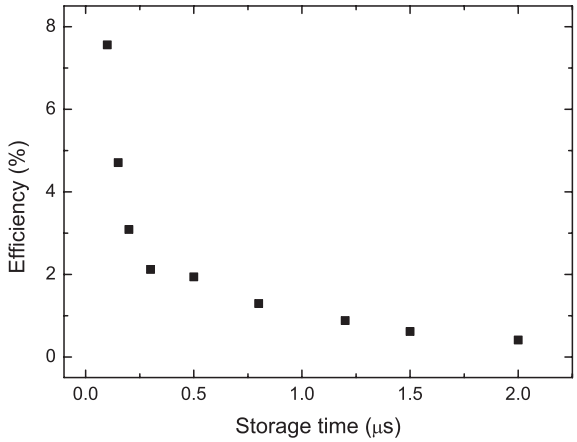

FIG. 4. The storage efficiency as a function of storage time. The storage sequence is repeated 400 times at a frequency of 400 kHz.

0.997, 1, and 0.999 for H, V, R, and D, respectively. Note that no dark counts of SPD are corrected through our experiment. Our results are far beyond the $2/3$ bound, which is the maximum average fidelity that can be achieved with a classical memory [29]. Controlled reversible inhomogeneous broadening (CRIB) [9,10,13] is a protocol that is similar to AFC. CRIB uses an external field to rephase the atoms and thus eliminates any classical light during the storage cycle; therefor, it should achieve a similar fidelity performance. Our scheme is applicable to the CRIB protocol.

By carefully designing the optical setup, we have eliminated most of the noise from the setup or the environment. The remaining imperfections are mostly introduced by the statistical photon drift and detector noise. We have also characterized our memory by measuring the read-write fidelity as a function of the storage time. The process fidelity shows little dependence on the storage time. For a longer storage time (500 ns), the fidelity decreases to 0.981 ± 0.003. Because the storage efficiency decreases quickly (as shown in Fig. 4), the signal to noise ratio decreases. This factor account for most of the degradation. In general, the echo-type memory based on collective interference is not sensitive to decoherence, although the efficiency degrades significantly. This phenomenon is elucidated by results showing that most of the atoms that are decohered do not contribute to the collective interference, as has been observed in classical photon-echo memory [30]. Our low-noise scheme should enable accurate experimental investigations into the influence of decoherence on memory fidelity.

We have demonstrated an ultrareliable quantum memory for photonic polarization-qubit in solids. By performing quantum process tomography, we measure the process fidelity for a 200 ns storage time with single-photon-level input pulses at 0.999 ± 0.002. This excellent fidelity performance should make the quantum memory suitable for quantum error-correction applications in large-scale quantum computation [31,32]. Moreover, the absence of ions' motion in the solid state means that even complex spatial structures can be generated by light and stored. Our results should produce solid-state devices that are capable of functioning as a quantum memory for light's polarization, temporal, and spatial information.

We note that related results have been obtained by two other groups [33,34]. Compared with their results, our quantum memory is compact and has ultrahigh fidelity.

This work was supported by the National Basic Research Program (2011CB921200), National Natural Science Foundation of China (Grant No. 60921091 and No. 10874162).

*cfli@ustc.edu.cn

[1] A. I. Lvovsky, B. C. Sanders, and W. Tittel, Nature Photon. **3**, 706 (2009).
[2] L.-M. Duan, and C. Monroe, Rev. Mod. Phys. **82**, 1209 (2010).
[3] D. N. Matsukevich and A. Kuzmich, Science **306**, 663 (2004).
[4] K. S. Choi, H. Deng, J. Laurat, and H. J. Kimble, Nature (London) **452**, 67 (2008).
[5] H. Tanji, S. Ghosh, J. Simon, B. Bloom, and V. Vuletić, Phys. Rev. Lett. **103**, 043601 (2009).
[6] H. Zhang, X. M. Jin, J. Yang, H. N. Dai, S. J. Yang, T. M. Zhao, J. Rui, Y. He, X. Jiang, F. Yang, G. S. Pan, Z. S. Yuan, Y. Deng, Z. B. Chen, X. H. Bao, S. Chen, B. Zhao, and J. W. Pan Nature Photon. **5**, 628 (2011).
[7] H. P. Specht, C. Nölleke, A. Reiserer, M. Uphoff, E. Figueroa, ,S. Ritter, and G. Rempe, Nature (London) **473**, 190 (2011).
[8] M. Lettner, M. Mücke, S. Riedl, C. Vo, C. Hahn, S. Baur, J. Bochmann, S. Ritter, S. Dürr, and G. Rempe, Phys. Rev. Lett. **106**, 210503 (2011).
[9] M. Hosseini, B. M. Sparkes, G. Hétet, J. J. Longdell, P. K. Lam, and B. C. Buchler, Nature (London) **461**, 241 (2009).
[10] M. Hosseini, G. Campbell, B. M. Sparkes, P. K. Lam, and B. C. Buchler, Nature Phys. **7**, 794 (2011).
[11] S. Olmschenk, D. N. Matsukevich, P. Maunz, D. Hayes, L.-M. Duan, and C. Monroe, Science **323**, 486 (2009).
[12] J. J. Longdell, E. Fraval, M. J. Sellars, and N. B. Manson, Phys. Rev. Lett. **95**, 063601 (2005).
[13] M. P. Hedges, J. J. Longdell, Y. Li, and M. J. Sellars, Nature (London) **465**, 1052 (2010).
[14] I. Usmani, M. Afzelius, H. de Riedmatten, and N. Gisin, Nature Commun. **1**, 12 (2010).
[15] M. L. Bonarota, J.-L. Gouët, and T. Chanelière, New J. Phys. **13**, 013013 (2011).
[16] E. Saglamyurek, N. Sinclair, J. Jin, J. A. Slater, D. Oblak, F. Bussières, M. George, R. Ricken, W. Sohler, and W. Tittel, Nature (London) **469**, 512 (2011).
[17] C. Clausen, I. Usmani, F. Bussières, N. Sangouard, M. Afzelius, H. de Riedmatten, and N. Gisin, Nature (London) **469**, 508 (2011).

[18] Y. F. Huang, B. H. Liu, L. Peng, Y. H. Li, L. Li, C. F. Li, and G. C. Guo Nature Commun. **2**, 546 (2011).
[19] C. L. Salter, R. M. Stevenson, I. Farrer, C. A. Nicol, D. A. Ritchie, and A. J. Shields, Nature (London) **465**, 594 (2010).
[20] D. G. England, P. S. Michelberger, T. F. M. Champion, K. F. Reim, K. C. Lee, M. R. Sprague, X.-M. Jin, N. K. Langford, W. S. Kolthammer, J. Nunn, and I. A. Walmsley, arXiv:1112.0900 [J. Phys. B (to be published)].
[21] H. de Riedmatten, M. Afzelius, M. U. Staudt, C. Simon, and N. A Gisin, Nature (London) **456**, 773 (2008).
[22] M. Sabooni, F. Beaudoin, A. Walther, N. Lin, A. Amari, M. Huang, and S. Kröll, Phys. Rev. Lett. **105**, 060501 (2010).
[23] M. Afzelius *et al.* Phys. Rev. Lett. **104**, 040503 (2010).
[24] S. R. Hastings-Simon, M. Afzelius, J. Minář, M. U. Staudt, B. Lauritzen, H. de Riedmatten, and N. Gisin, Phys. Rev. B **77**, 125111 (2008).
[25] M. Afzelius, C. Simon, H. de Riedmatten, and N. Gisin, Phys. Rev. A **79**, 052329 (2009).
[26] See Supplemental Material at http://link.aps.org/supplemental/10.1103/PhysRevLett.108.190505 for details.
[27] I. L. Chuang and M. A. Nielsen, J. Mod. Opt. **44**, 2455 (1997).
[28] J. L. O'Brien, G. J. Pryde, A. Gilchrist, D. F. V. James, N. K. Langford, T. C. Ralph, and A. G. White, Phys. Rev. Lett. **93**, 080502 (2004).
[29] S. Massar and S. Popescu, Phys. Rev. Lett. **74**, 1259 (1995).
[30] M. U. Staudt, M. Afzelius, H. de Riedmatten, S. R. Hastings-Simon, C. Simon, R. Ricken, H. Suche, W. Sohler, and N. Gisin, Phys. Rev. Lett. **99**, 173602 (2007).
[31] T. D. Ladd, F. Jelezko, R. Laflamme, Y. Nakamura, C. Monroe, and J. L. O'Brien, Nature (London) **464**, 45 (2010).
[32] D. S. Wang, A. G. Fowler, and L. C. L. Hollenberg, Phys. Rev. A **83**, 020302(R) (2011).
[33] C. Clausen, F. Bussières, M. Afzelius, and N. Gisin, this issue, Phys. Rev. Lett. **108**, 190503 (2012).
[34] M. Gündoğan, P. M. Ledingham, A. Almasi, M. Cristiani, and H. de Riedmatten, preceding Letter, Phys. Rev. Lett. **108**, 190504 (2012).